Dimensional Changes of ProRoot white Mineral Trioxide Aggregate, EndoSequence Root Repair Material, and Biodentine During Setting Using Digital Image Correlation

A Thesis
SUBMITTED TO THE FACULTY OF
UNIVERSITY OF MINNESOTA
BY

Amber Jean Zedler DDS

IN PARTIAL FULFILLMENT OF THE REQUIREMENTS
FOR THE DEGREE OF
MASTER OF SCIENCE

Dr. Scott McClanahan, Dr. Samantha Roach, Dr. Alex Fok

September 2016

Acknowledgements

Thank you to Dr. McClanahan for your incredible dedication and sacrifice to make each of us the best endodontist that we can be.

Thank you to Drs. Roach, Barsness, and Rodriguez for your knowledge, support, and enthusiasm through this academic Olympic adventure!

Dr. Doyle, Dr. Edmunds, Dr. Ryan, Dr. Spitzmueller, and Dr. Zucker: Thank you for giving of your time and passion for endodontics.

To my fellow residents: It has been an unforgettable adventure; thank you for your friendship, encouragement, and much laughter during this residency.

To the assistants and staff: It was a pleasure working with you, and we could not do it without you.

Dedication

This thesis is dedicated to my incredible family; your support never wavered.

Thank you to my father who taught me the value of hard work and persistence. Thank you to my mother for teaching me love without bounds, and being a living example.

Table of Contents

List of Tables

List of Figures

Introduction

Endodontics is the prevention and treatment of apical periodontitis. The root canal system of a tooth may be thought of as containing generally one to four canals that extend from the pulp chamber to the apices. The reality is that this system is a network of fins and isthmuses between a varying number of canals. The complexity of the anatomy presents challenges in cleaning and shaping the root canal that cannot be perfectly addressed by our current best mechanical and chemical debridement methodologies.

When there is persistence of apical periodontitis after root canal therapy, the clinician must consider the possible presence of anatomic complexities that cannot be managed with orthograde endodontic treatment. Endodontic microsurgery can be an appropriate treatment to eradicate the etiology of persistent periradicular disease. Root end surgery consists of resection and root end filling and can give the clinician the ability to remove and seal off the complex terminus of the canals and their ramifications. An appropriate root end filling material is a critical element for the surgical procedure.

Dimensional changes in the repair material could enhance or weaken the seal of the root end filling. A slight expansion of the material may aid in its sealing properties, as well as reduce marginal discrepancies; however, substantial expansion could pose an increased risk of root fractures at the resected root end. In contrast to expansion, shrinkage could lead to marginal breakdown of the root end filling material and result in leakage. Expansion has been measured in gray and white mineral trioxide aggregate (MTA) by Storm et al. (2008) with the experimental samples immersed in water or

Hank's Balanced Salt Solution. The current study aims to quantify and compare the dimensional changes of ProRoot white MTA, EndoSequence Root Repair Material (ERRM), and Biodentine in a simulated root end model using a novel approach: digital image correlation of the materials as they set.

Literature Review

Root Canal Objective

It has been well established that apical periodontitis is caused by bacteria (Kakehashi et al., 1965). Root canal treatment strives to remove the bacteria in the canal, and prevent bacterial recolonization or regrowth. Dr. Schilder (1974) presented four important biological objectives for nonsurgical root canal treatment: 1) procedures should be confined to the roots themselves, 2) necrotic debris should not be forced beyond the foramina, 3) all tissues should be removed from the root canal space, and 4) sufficient space for intracanal medicaments and irrigation should be created (Schilder, 1974). Iatrogenic errors can and do occur during endodontic treatment, even with the most masterful clinician.

Errors in preparation

Addressing the etiology is essential for healing to occur after endodontic treatment. Removal of the bacteria in the apical 3mm, or the "critical zone", is crucial to the success of endodontic treatment (Simon, 1994). Procedural errors, such as formation of a ledge, can prevent adequate cleaning and shaping of the critical zone, by preventing us from accessing this area (Jafarzadeh and Abbott, 2007). The cleaning and shaping procedures performed on the tooth alter the original anatomy of the canal: creation of an elbow, or an apical zip. An apical zip makes an ideal obturation more difficult to achieve (Weine et al., 1975). Over instrumenting or over enlarging the canal may lead to a strip perforation on the furcation side, the danger zone, of the roots of molar teeth (Abou-Rass

et al, 1980; Harris et al. 2013). Accidental perforations occur in approximately 2-12% of endodontically treated teeth (Tsesis and Fuss, 2006). Any perforation of the natural dental anatomy can lead to secondary inflammatory periodontal involvement and loss of attachment (Frank, 1974). The prognosis of a tooth with a root perforation depends on the time between the occurrence of the perforation and repair of the perforation, location and size of the perforation, and the sealability of the repair material. While it would be best to avoid such procedural errors, if they do occur, the clinician should repair the defect as quickly as possible and with the best available material (Alhadainy, 1994).

Historic materials for perforation repair

Nearly every material available in the dental armamentarium has been tried as a perforation repair material. Historically, root perforations have been obturated with amalgam or gutta-percha. Amalgam was found to be more successful than gutta-percha with a 54% success overall when used for repairing a perforation. Of the perforation repairs that failed, 69% occurred when the repair materials were extruded beyond the root surface (Benenati et al., 1986). In an effort to keep the repair material inside the tooth, Lemon (1992) described an internal matrix technique of a hydroxyapatite barrier to allow shaping of the repair material to follow the contour of the natural tooth surface. A modified matrix technique was later presented using a collagen matrix and gray MTA (Bargholz, 2005). Gray MTA has been shown to cause less inflammation as a perforation repair material than amalgam (Pitt Ford et al., 1995).

Surgery

When apical periodontitis persists despite the clinician's best efforts at cleaning and shaping, disinfection, and obturation, surgery may provide another way to remove the etiology. Indications for an apical microsurgery may include: persistent periapical radiolucency, persistent pain or swelling, procedural errors, presence of a post and crown, calcified canals, separated instruments, failed traditional surgery, overfilling of the canal with periapical radiolucency, and complex apical anatomy that was inaccessible during the orthograde treatment (AAE, 2010). The advent of the surgical microscope has increased our clinical visualization and thus our ability to conservatively and successfully treat apical pathology with microsurgery (Kim and Kratchman, 2006).

Amalgam as a root end filling material historically

Amalgam has a long history of use as a root-end filling material prior to the introduction of gray MTA. In a dog study, histopathological examination of periradicular tissues of roots that were filled with amalgam all had moderate to severe inflammation. At 2- to 5-weeks post-surgery, polymorphonuclear leukocytes were the predominant inflammatory cells in the periradicular tissues. No fibrous capsule tissue was found over the amalgam, and no cementum formation was observed. In the same study, gray MTA was found to have more favorable healing results (Torabinejad et al., 1995). In a cytotoxicity study, amalgam had a larger cell-free zone, and thus higher cytotoxicity, than Super-EBA and IRM in cultures of human PDL cells and cultures of human osteoblast-like cells (Zhu et al., 1999).

Mineral Trioxide Aggregate

ProRoot gray MTA (Dentsply Tulsa Dental Specialties, Johnson City, TN) is primarily composed of tricalcium silicate, dicalcium silicate, and bismuth oxide, with smaller amounts of tricalcium aluminate and tetracalcium aluminoferrite. ProRoot white MTA (Dentsply Tulsa Dental Specialties, Johnson City, TN) does not have the tetracalcium aluminoferrite. Both white and gray MTA have a similar chemical composition as does Portland cement, with the addition of bismuth oxide as a radiopacifier (Camilleri et al., 2005). Portland cement also has potassium, which is not present in gray or white MTA (Song et al., 2006). Hydration of the tricalcium and dicalcium silicate produces calcium silicate hydrate gel and calcium hydroxide (Camilleri et al., 2005).

Gray and white MTA show biocompatibility, demonstrated by cell growth on either MTA that was cured for either 1 day or 28 days. The 1-day cure samples had a higher biocompatibility which may be due to a greater amount of calcium hydroxide produced in the earlier sample than in the 28-day set material (Camilleri et al., 2004). Both materials produce more calcium initially, followed by a decrease, and then a rise. The crystal precipitated on the surface of both were analyzed and found to be chemically and structurally similar to hydroxyapatite. There were significantly more crystals formed on the gray MTA, possibly lending a clinical advantage to gray MTA (Bozeman et al., 2006). A review of the literature by Camilleri and Pitt Ford (2006) found 53 studies that have been published that support the biocompatibility of gray MTA. The hydration reactions of the tricalcium silicate and the dicalcium silicate are:

$$2(3CaO{\cdot}SiO_2) + 6H_2O \rightarrow 3CaO{\cdot}2SiO_2{\cdot}3\ H_2O + 3Ca(OH)_2$$

$$2(2CaO{\cdot}SiO_2) + 4H_2O \rightarrow 3CaO{\cdot}2SiO_2{\cdot}3\ H_2O + Ca(OH)_2$$

The result is a poorly crystalized and porous solid. The bismuth oxide was found to also be part of the calcium silicate hydrate (Camilleri, 2007). The initial surge of calcium release is due to the production of calcium hydroxide during the hydration reaction. A slower secondary release of calcium comes from decomposition/decalcification of the calcium silicate hydrate over time (Camilleri, 2008).

Gray MTA has a mean setting time of 2 hours and 45 minutes, as tested by a Gilmore needle. Gray MTA material is basic when mixed, 10.2 pH, and becomes more basic as it sets, 12.5 pH at 3 h. (High pH may induce hard tissue formation as with the use of calcium hydroxide). Hydration of gray MTA powder forms a colloidal gel that solidifies to a hard structure in less than 3 hours (Torabinejad et al., 1995).

Characteristics of an ideal root end filling material include a material that is well tolerated by periapical tissues, is bactericidal or bacteriostatic, adheres to the tooth, dimensionally stable, readily available and easy to handle, does not stain teeth or periradicular tissue, is noncorrosive, resistant to dissolution, electrochemically inactive, promotes cementogenesis, easy to use, and radiopaque (Kim, 2001). Gray MTA has become the gold standard for root end fillings (Johnson, 1999). Physical properties of white MTA include a long setting time, high pH, low compressive strength, antibacterial and antifungal properties (Parirokh and Torabinejad, 2010pI). Gray MTA seals the apex well and is biocompatible (Torabinejad and Parirokh, 2010). Disadvantages of gray

MTA are a long setting time, high cost, and ability to cause discoloration (Parirokh and Torabinejad, 2010pIII).

EndoSequence Root Repair Material

Another more recently developed root end filling material is EndoSequence Root Repair Material (ERRM) from Brassler (Savanah, GA). According to the manufacturer, ERRM is composed of calcium silicates, monobasic calcium phosphate, zirconium oxide, tantalum oxide, proprietary fillers, and thickening agents. The second generation ERRM is a premixed "fast set" material that comes as a putty in a syringe. It has a working time of greater than 30 minutes and a setting time of 4 hours. ERRM is a bioceramic material with good stability, high mechanical dentin bond strength, high pH, radiopaque, hydrophilic setting, and it comes premixed (Hirschman, 2012). ERRM showed similar cell viability to gray MTA and white MTA when fresh or set for 72 hours (AlAnezi et al., 2010). Ma et al. (2011) also found ERRM putty and paste to have similar *in vitro* biocompatibility as gray MTA, when assessing cell viability and adhesion.

In a study on the antibacterial activity of ERRM paste, ERRM putty, and white MTA against *E. faecalis*, it was found that all 3 materials possessed antibacterial properties during their setting period and that there was no difference between the materials in their antibacterial efficacy (Lovato and Sedgley, 2011). A smaller particle size contributes to more favorable handling properties of the EndoSequence materials compared to gray MTA. ERRM gets its high mechanical bond strength due to small particles being able to enter the dentin tubules, and its high pH contributes to its

antibacterial benefits (Damas et al., 2011). White MTA and ERRM are bioactive, forming apatite precipitates on their surfaces after exposure to simulated tissue fluid (phosphate-buffered saline) (Shokouhinejad et al., 2012).

The osteogenic potential of gray MTA and ERRM were compared by using a 3-dimensional culture system. A 3-dimensional scaffold was placed on gray MTA or ERRM that had set for 48 hours, and mouse osteoblasts were grown on the scaffold. Alkaline phosphatase and bone sialoprotein expression from the osteoblasts was increased significantly more from the ERRM samples compared to the gray MTA samples. Greater osteoblast differentiation occurred in the presence of ERRM vs. gray MTA (Rifaey et al., 2016). An *in vivo* dog study showed healing after root-end surgery in teeth treated with gray MTA and ERRM. However, the ERRM groups achieved a better tissue healing response adjacent to the root-end as evidenced by increased formation of cementum-like tissue, periodontal ligament-like tissue, and bone compared to gray MTA (Chen et al., 2015).

A comparison between white MTA and ERRM pH changes was made by simulating external resorption defects on human teeth and then filling the root canals with one of the experimental materials. The pH measurements were not different at the beginning, but after 24 hours the white MTA group had a significantly higher pH (8.79 vs. 8.56) than the ERRM group. The pH for both groups decreased over time and at the 4-week time point, both were similar to the negative control. The authors suggest that for ERRM, the decrease in the pH between 24 hours and 1 week might be attributable to the final cure of the material. According to the manufacturer, gray MTA, although set at 4

hours, requires approximately 4 weeks for a full cure of the material (Hansen et al., 2011).

Walsh et al. (2014) studied the compressive strength of hydraulic silicate-based root-end filling materials, including white MTA and ERRM, in the presence of saline and fetal bovine serum. ERRM showed significantly higher compressive strength than white MTA. White MTA has a significantly lower compressive strength when exposed to fetal bovine serum rather than saline. ERRM showed a minimal effect from fetal bovine serum vs. saline. ERRM showed expansion above the mold used in this study, in both the group exposed to fetal bovine serum, and exposed to saline. This expansion was not measured (Walsh et al., 2014).

Biodentine

Biodentine (Septodont, Cambridge, ON, Canada) is another new product. Biodentine is a calcium-silicate based material containing: tricalcium silicate, calcium carbonate, and zirconium oxide, and a water-based liquid-containing calcium chloride as the setting accelerator and a water-reducing agent (hydro-soluble polymer) that comes in a ready-to-mix capsule (Septodont scientific file). Set Biodentine is composed of tricalcium silicate, calcium carbonate, zirconium oxide, and calcium hydroxide. Biodentine samples immersed in Hank's Balanced Salt Solution for 28 days released calcium hydroxide as evidenced by calcium ions in the leachate. The calcium levels were maintained until 28 days. The pH of the solution was alkaline, remaining at 12 at all-time points from 1 to 28 days (Grech et al., 2013a).

Biodentine has an initial set time of 9-12 minutes when tested according to the ISO standard with the Gilmore needle, after which it is acceptable to place a permanent restoration (Biodentine scientific file, 2010). Biodentine has a quicker setting time than gray or white MTA due to the calcium chloride in the Biodentine liquid. Biodentine has a low water-to-cement ratio because of the addition of a water soluble polymer. The low water content increases the strength of the cement. The setting time of Biodentine was tested with Biodentine samples immersed in Hank's Balanced Salt Solution while setting. Biodentine had a final set at 45 minutes as evaluated by a modified Vicat apparatus: set was determined as the time when a weighted needle failed to make an indent in the surface (Grech et al., 2013b).

Biodentine and white MTA are not significantly different in regards to their cytotoxicity, and both are less cytotoxic than glass ionomer cement (Zhou et al., 2013). Biodentine has fast setting, good sealing properties, and is bioactive (Zanini et al., 2012). Compared to MTA Angelus, Biodentine produced less calcium hydroxide. Both materials allowed the deposition of hydroxyapatite on their respective surfaces when soaked in Hank's Balanced Salt Solution (Camilleri et al., 2013).

Digital Image Correlation

Digital image correlation (DIC) is a non-contact optical method used to measure strain and displacement. DIC compares photographs of a subject matter during different stages of deformation. Many of the surfaces imaged with this technology have enough texture naturally without the need for any special surface preparation. Concrete is one

example of a material analyzed by DIC, and which needs no additional surface preparation. Surface deformation can be measured by this method down to one part per million of the field of view (McCormick and Lord, 2010). DIC can measure microscopic strain distribution at the grain level in dual phase steels using SEM topography image correlation. Heat treatment changes the microscopic distribution of strain between martensite and ferrite phases, and this can be measured by DIC (Kang et al., 2009).

Chuang et al. (2008) described the use of Digital Image Correlation for measuring shrinkage of composite resins. Li et al. (2009(a)) measured polymerization shrinkage of composite resins with DIC. The composite surface was sprayed with a fine layer of black paint in order to create irregular-shaped speckles on the surface. The speckles are then tracked and analyzed by the image correlation system. Li et al. (2009(b)) also compared this with other assessments of parameters of composites. Composite shrinkage has subsequently been evaluated by Chuang et al. (2011), Li et al. (2014), and Lau et al. (2015). These studies all used a single camera Digital Image Correlation. Miletic et al. (2011) made a 3D Digital Image Correlation by using 2 cameras for the analysis.

Composite shrinkage studies have used molds of stainless steel (Li et at., 2009; Lau et al., 2015), glass (Li et al., 2014), Teflon (Miletic et al., 2011), and human teeth (Chang et al., 2011). The surfaces were coated with a thin layer of black paint (Miletic et al., 2011; Li et al., 2009), a thin layer of white paint followed by black charcoal powder (Li et al., 2014; Lau et al., 2015), speckled with titanium oxide powder (Chuang et al., 2011), or left uncoated (Li et al., 2009).

Specific Aims

This study attempts to address the following questions:

1. What are the dimensional changes of white Mineral Trioxide Aggregate, EndoSequence Root Repair Material, and Biodentine in a simulated root end model during setting of the respective materials?
2. Is there a difference between the dimensional changes of the three materials?

Null Hypothesis

The null hypothesis states that there are no differences in dimensional changes between the three materials.

Materials and Methods

Sample Preparation

The materials tested were white MTA, EndoSequence Root Repair Material, and Biodentine; see Figure 1. A sample size of 10 in each group (30 total) will have 82% power to detect a difference in mean expansion of 1.5 standard deviations between materials using a one-way ANOVA with a 0.05 level of significance. Ten samples of each material were prepared according to the manufacturer's directions, except for the ERRM which comes ready to use in a syringe. The white MTA was mixed on a glass slab: a 1-gram packet of the powder and the supplied ampule of water, reported to be 0.35 grams by the manufacturer. If the mix was too dry to incorporate all of the powder, 1-2 drops of additional sterile water was added as described in the mixing instructions. Each Biodentine capsule had five drops of the provided liquid added, before mixing in an amalgamator at 4000±200 rpm (rabbit setting), for 30 seconds.

Figure 1

Teflon was used to fabricate the experimental molds in this study, similar to the cylinders used in the composite shrinkage study by Miletic et al. (2011). The Teflon molds were cylindrical with an internal diameter of 4 mm, and an external diameter of

6mm (1mm width of the Teflon ring). The height was 4mm, for a volume of 50.27mm^3 within the mold. The respective materials were placed into the molds with a carrier and hand condensed to be flush with the top of the mold, to simulate a clinically placed root end filling. Concrete can be imaged with no surface treatment. However, the smaller particle size of the bioceramic materials requires additional texture for the camera to track distortion. The surface of the material was sprayed with a fine charcoal powder; see Figure 3. The carbon particles provided points for the software to track in order to measure the dimensional changes. A pilot study with gray MTA revealed inadequate contrast between the gray MTA and the carbon particles. White MTA was selected over gray in this study for this reason.

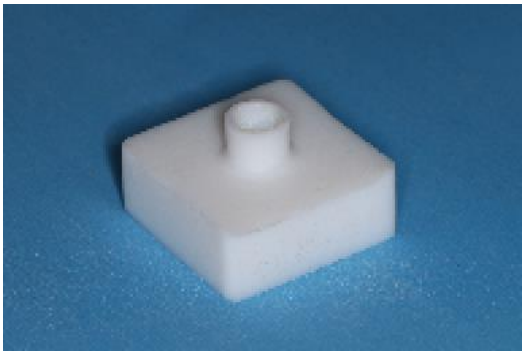

Figure 2: Teflon mold

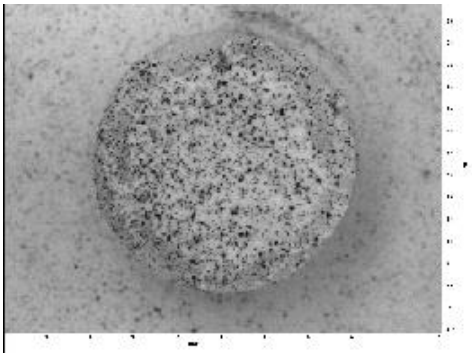

Figure 3: Carbon particles on white MTA

The experimental time for the white MTA was set at 4 hours to exceed the set time given by the manufacturer and based on a pilot study where there was minimal expansion in samples analyzed at twelve hours as compared to four hours. A pilot study on the EndoSequence Root Repair Material found that the material had not reached a complete set at the manufacturer reported 4 hour set time. When the ERRM was observed for increased time, at 5 hours and at 6 hours, there was a sheen on the surface of the material. It is unknown what caused the sheen, but the light reflection from this

surface sheen in the images taken with the camera created distortion in the analysis of the samples. The experimental time was set at 4 hours, which was when the final accurate image could be taken. The experimental time for the Biodentine samples was set based on the evaluation by Grech et al. (2013b), measuring the set with a modified Vicat apparatus.

Imaging

Samples were imaged using a CCD camera (Point Gray Grasshopper GRAS-20S4C-C) at initial mix, and at 15, 30, 45, and 60 minutes. The white MTA and ERRM samples were also imaged at 120, 180, and 240 minutes. The samples were kept in a high humidity (>80%) room temperature environment during the setting period. The humidity was maintained by 2 saturated cotton rolls near the sample. The sample and cotton rolls were covered with a plastic container between images. The camera and Teflon mold were fixed in place to avoid any movement between images; see Figure 4. A calibration image was taken for each sample.

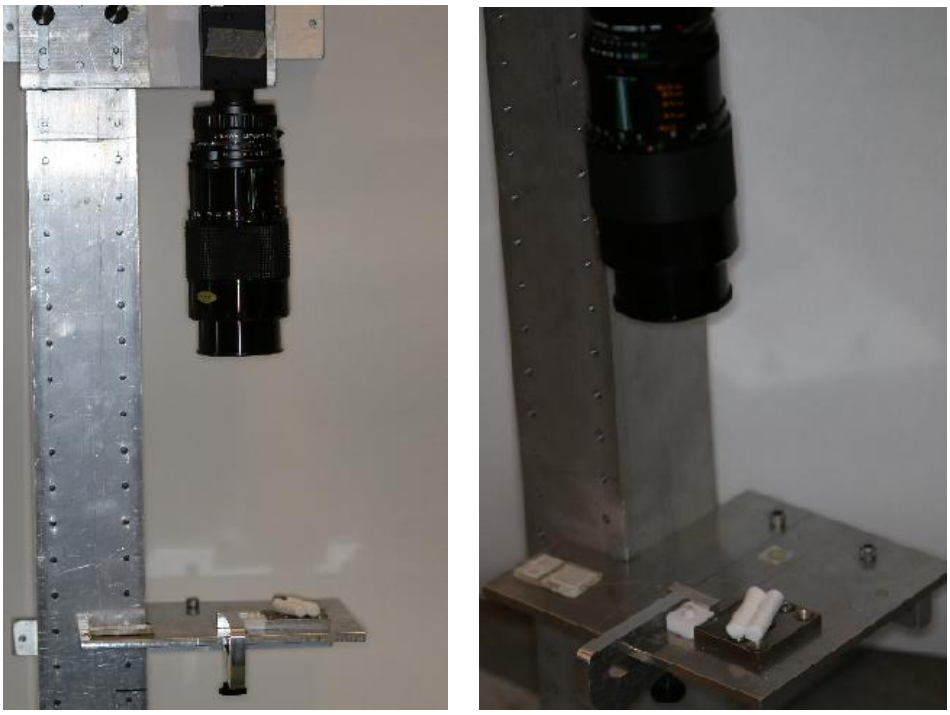

Figure 4

Analysis

The images were analyzed with digital image correlation using DaVis software (LaVision GmbH, Germany). The software measures the movement of the carbon particles on the surface of the material as it sets over time. The dimensional changes were measured in the x- and y-axis. Two-dimensional strain was calculated in the xy plane over a 4 mm diameter circle, an area of 12.56 mm^2. Descriptive statistics were used to summarize the outcomes by material and time. A time by material interaction was tested to compare slopes between materials using a mixed model with strain measure as the outcome, time (continuous) and material as fixed effects, and sample as a random effect. P-values less than 0.05 were considered statistically significant. SAS V9.3 was used for the analysis.

Results

The strain in the x-axis, Exx, and that in the y-axis, Eyy, was calculated for each material including Biodentine (Table 10 in Appendix) at each time point: 15, 30, 45, and 60 minutes, and for white MTA (Table 8 in Appendix) and ERRM (Table 9 in Appendix) at 120, 180, and 240 minutes also. Two-dimensional strain was calculated and the results are tabulated in Table 1 for white MTA, Table 2 for ERRM, and Table 3 for Biodentine. Figures 5-7 show the deformation visually as computed by the digital image correlation software for each respective material.

The white MTA and Biodentine samples all demonstrated shrinkage. The white MTA shrinkage was from 0.86% to 2.98%, with a mean of 1.84% and standard deviation of 0.61%. At 4 hours, the dimensional changes of the white MTA appear to have leveled off and are changing minimally (Figure 5, Table 1). Biodentine shrinkage was from 0.43% to 1.88%, with a mean of 1.30% shrinkage and standard deviation of 0.42% (Figure 6, Table 2). The ERRM expanded from 0.17% to 2.56%, with a mean of 1.23% and a standard deviation of 0.88%, with all samples demonstrating expansion (Figure 7, Table 3).

White Mineral Trioxide Aggregate

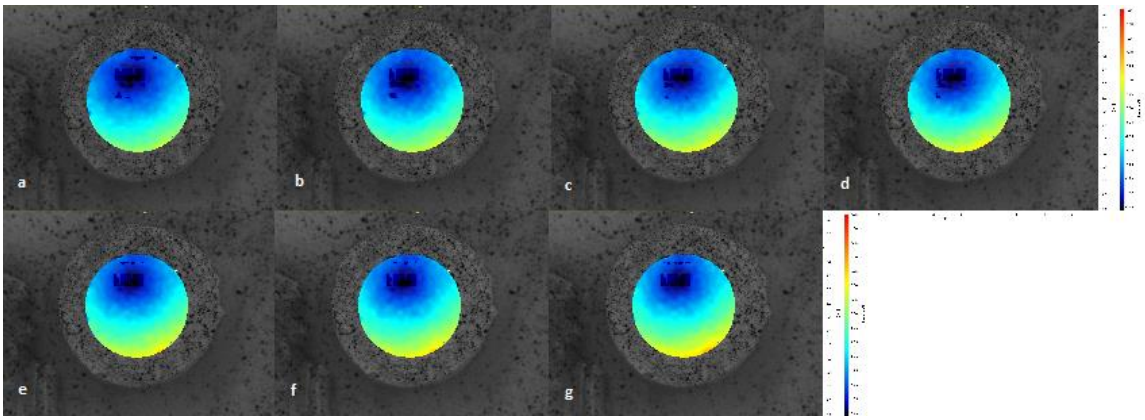

Figure 5: White MTA strain at a) 15 min, b) 30 min, c) 45 min, d) 60 min, e) 120 min, f) 180 min, and g) 240 min.

MTA 2D strain: Exx+Eyy (%)

Time (min)	1	2	3	4	5	6	7	8	9	10
15	-0.63160		-2.79272	-2.02063	-2.15388	-1.139987	-1.636430	-1.468410	-1.468410	-1.054126
30	-0.73084	-1.50673	-2.89578	-2.17784	-2.29692	-1.224813	-1.813672	-1.570874	-1.570874	-1.218192
45	-0.77735	-1.63965	-2.89894	-2.21383	-2.31733	-1.229656	-1.826838	-1.676067	-1.676067	-1.228412
60	-0.80401	-1.66467	-2.9275	-2.31358	-2.3356	-1.273674	-1.735179	-1.616254	-1.616254	-1.190521
120	-0.83952	-1.68055	-2.96618	-2.2531	-2.40151	-1.286757	-1.865619	-1.399412	-1.655982	-1.332819
180	-0.85404	-1.72604	-2.96493	-2.28459	-2.40211	-1.325096	-1.951286	-1.653991	-1.704542	-1.363593
240	-0.85793	-1.7472	-2.97951	-2.30856	-2.42137	-1.312934	-2.019364	-1.707608	-1.707608	-1.371848

Table 1: Two dimensional strain, Exx + Eyy strain, as computed for each time point for each white MTA sample. *Note: in sample 2, at 15 min, the computer froze and the image was not recorded.

EndoSequence Root Repair Material

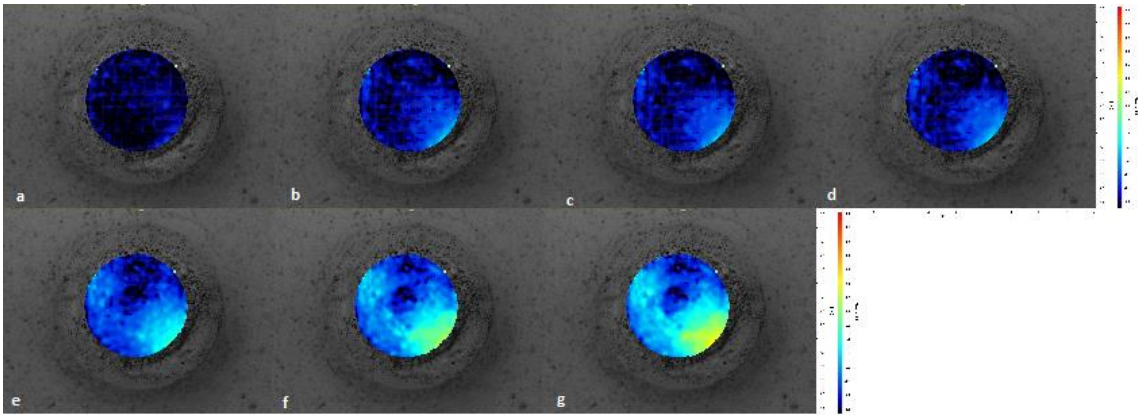

Figure 6: ERRM strain at a) 15 min, b) 30 min, c) 45 min, d) 60 min, e) 120 min, f) 180 min, and g) 240 min.

ERRM 2D Strain: Exx+Eyy (%)

Time (min)	1	2	3	4	5	6	7	8	9	10
15	0.08601	0.141557	0.08651	-0.00737	0.1494373	0.064756	0.223579	0.101025	0.356264	0.170409
30	0.11556	0.19931	0.165673	-0.03701	0.1149453	0.108495	0.456684	0.160551	0.528074	0.453419
45	0.11472	0.22222	0.214689	0.115206	0.1368919	0.171779	0.616136	0.215433	0.589395	0.480956
60	0.10198	0.295396	0.287148	0.084863	0.1165918	0.093256	0.767812	0.41209	0.657935	0.48972
120	0.1139	0.367439	0.620851	0.172751	0.2043129	0.210659	1.249958	1.033841	1.293316	0.805947
180	0.13862	0.49366	1.123302	0.292854	0.300143	0.277515	2.065165	1.866898	1.664563	1.309779
240	0.17318	0.883785	1.533514	0.464395	0.412465	0.481814	2.55509	2.4808	1.903085	1.373348

Table 2: Two dimensional strain, Exx + Eyy strain, as computed for each time point for each ERRM sample.

Biodentine

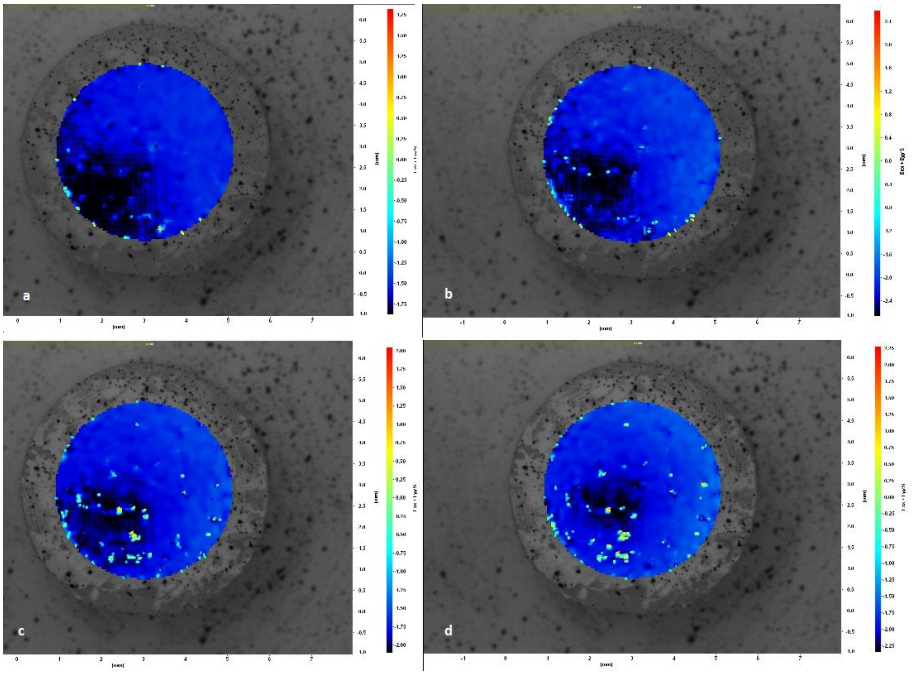

Figure 7: Biodentine strain at a) 15 min, b) 30 min, c) 45 min, d) 60 min.

Biodentine 2D strain: Exx+Eyy (%)

Time (min)	1	2	3	4	5	6	7	8	9	10
15	-0.449335	-0.531787	-0.547563	-0.443949	-0.776299	-0.297977	-0.34674	-0.516014	-0.218412	-0.062981
30	-0.534771	-1.132657	-1.012096	-0.696844	-1.250955	-0.560746	-0.55051	-0.501392	-0.674378	-0.12689
45	-0.936295	-1.248493	-1.444295	-0.970796	-1.533222	-0.821364	-0.941823	-0.950235	-1.237817	-0.224707
60	-1.208612	-1.280464	-1.733168	-1.159891	-1.878217	-0.967761	-1.305842	-1.412097	-1.645899	-0.426486

Table 3: Two dimensional strain, Exx + Eyy strain, as computed for each time point for each Biodentine sample.

Statistical Analysis

The following table contains analysis of the data including minimum, maximum, mean and standard deviation, and median at each time point for the three materials.

Analysis Variable: Outcome Outcome									
Group	**Time**	**N Obs**	**N**	**N Miss**	**Mean**	**Std Dev**	**Median**	**Minimum**	**Maximum**
Biodentine	0	10	10	0	0.0000	0.0000	0.0000	0.0000	0.0000
	15	10	10	0	-0.4191	0.1985	-0.4466	-0.7763	-0.0630
	30	10	10	0	-0.7041	0.3376	-0.6176	-1.2510	-0.1269
	45	10	10	0	-1.0309	0.3703	-0.9605	-1.5332	-0.2247
	60	10	10	0	-1.3018	0.4158	-1.2932	-1.8782	-0.4265
	120	10	0	10	.	.	.	.	.
	180	10	0	10	.	.	.	.	.
	240	10	0	10	.	.	.	.	.
ERRM	0	10	10	0	0.0000	0.0000	0.0000	0.0000	0.0000
	15	10	10	0	0.1372	0.0996	0.1213	-0.0074	0.3563
	30	10	10	0	0.2266	0.1863	0.1631	-0.0370	0.5281
	45	10	10	0	0.2877	0.1963	0.2151	0.1147	0.6161
	60	10	10	0	0.3307	0.2468	0.2913	0.0849	0.7678
	120	10	10	0	0.6073	0.4612	0.4941	0.1139	1.2933
	180	10	10	0	0.9532	0.7399	0.8085	0.1386	2.0652
	240	10	10	0	1.2261	0.8779	1.1286	0.1732	2.5551
White MTA	0	10	10	0	0.0000	0.0000	0.0000	0.0000	0.0000
	15	10	9	1	-1.5962	0.6509	-1.4684	-2.7927	-0.6316
	30	10	10	0	-1.7007	0.6232	-1.5709	-2.8958	-0.7308
	45	10	10	0	-1.7484	0.6124	-1.6761	-2.8989	-0.7774
	60	10	10	0	-1.7477	0.6258	-1.6405	-2.9275	-0.8040
	120	10	10	0	-1.7681	0.6255	-1.6683	-2.9662	-0.8395
	180	10	10	0	-1.8230	0.6072	-1.7153	-2.9649	-0.8540
	240	10	10	0	-1.8434	0.6140	-1.7274	-2.9795	-0.8579

Table 4: Descriptive statistics: The MEANS procedure

Comparison of slopes (strain vs time) between Materials

The slopes of the strain during setting of the three materials were compared and there was a significant difference between the slopes (Table 5). Analysis between pairs of the slopes indicates that there was a significant difference between each of the slopes (Table 6). Figure 8 is a graph of the strain versus time of each material with each of the data points plotted. The estimated slope of each material is graphed. When comparing the group means, there was significant difference between the means at each time point up to 60 minutes (Table 7).

Comparison	P-value†
White MTA vs ERRM vs Biodentine	<0.0001 *

Table 5

† Testing time by material interaction in a mixed model with strain measure as the outcome and time (continuous) and material as fixed effects and sample as a random effect. SAS V9.3 was used for the analysis.

*Indicates slopes are not the same (statistically significant at the 0.05 level);

Comparison	P-value
Estimated Biodentine slope (SE) = -0.020 (0.002)	p<0.0001, (testing slope versus 0)
Estimated ERRM slope (SE) = 0.005 (0.0003)	p<0.0001
Estimated white MTA slope (SE) = -0.001 (0.0003)	p=0.0134

Table 6: Analysis between pairs of estimated slopes of the line representing strain over time for each material

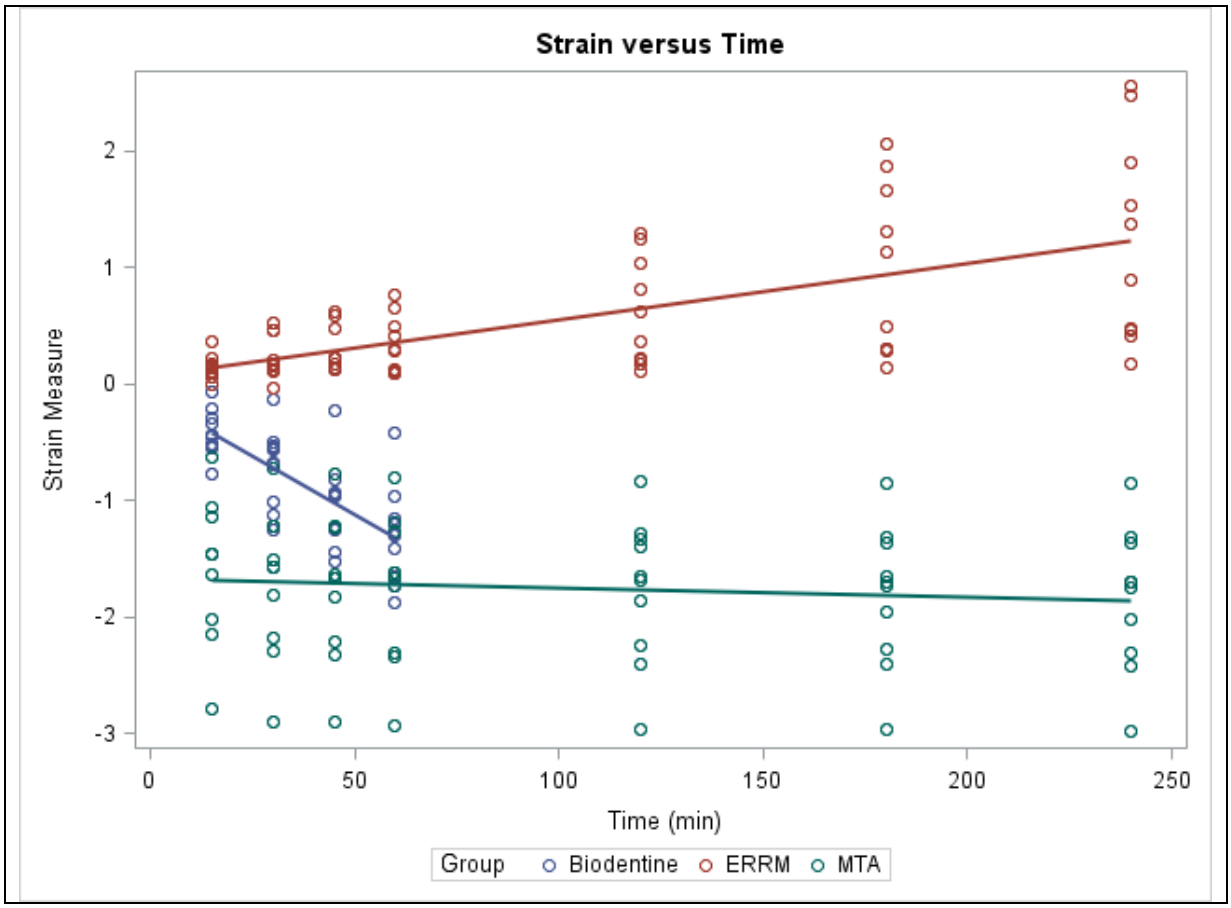

Figure 8: Graph of strain at each time point for each sample. The line represents the estimated slope of strain over time for each material.

Comparing group means at Specific Time points

Time	Biodentine	ERRM	white MTA	P-value†
15	-0.42 (0.16)	0.14 (0.16)	-1.58 (0.16)	<.0001
30	-0.70 (0.16)	0.23 (0.16)	-1.70 (0.16)	<.0001
45	-1.03 (0.16)	0.29 (0.16)	-1.75 (0.16)	<.0001
60	-1.30 (0.16)	0.33 (0.16)	-1.75 (0.16)	<.0001

Table 7: Means (SD) are in table. † From the mixed model, comparing means between groups.

Discussion

In the current study, white MTA and Biodentine demonstrated shrinkage on setting and ERRM demonstrated expansion. Previously white and gray MTA have been measured to expand during setting (Chng et al., 2005, Storm et al., 2008). Chng et al. (2005) measured mean expansion of gray and white MTA during setting to be 0.28%±0.09 and 0.30%±0.01 respectively using ISO 6876:2001 standards for dental root canal sealers. A 1-mm thick sample was placed in a ring with glass plates on the top and bottom, and any increase in distance between the two glass plates was measured when the material is set. The weight of the top glass plate may have affected the measurement and led to an underestimation of the expansion.

Storm et al. (2008) used a novel method to compare hygroscopic linear setting expansion of gray and white MTA, and Portland cement. A linear expansion measuring device was developed for Storm's study. The device consisted of a dilatometer and a nylon piston attached to a linear variable displacement transformer (LVDT). It is possible that the weight of the LVDT could have affected the measurement, leading to an underestimation of the expansion. A mold in the center measuring 10 mm in height and 5 mm in diameter held the material during setting. A computer recorded movement of the piston to measure volumetric expansion of the materials over 24 hours. The mean expansion of gray MTA was 0.47% at 300 minutes and 1.02% at 24 hours in water and 0.34% at 300 min and 0.68% at 24 hours in Hank's Balanced Salt Solution. The mean expansion of white MTA was 0.04% at 300 minutes and 0.08% at 24 hours in water and 0.09% at 300 minutes and 0.11% at 24 hours in Hank's Balanced Salt Solution. The

expansion of gray MTA was significantly more than the expansion of white MTA. The difference in expansion between submersion in water or Hank's Balanced Salt Solution was not statistically significant for either material.

Gandolfi et al. (2009) investigated the setting times and the linear expansion between the initial and final setting times of experimentally accelerated calcium-silicate cements and gray MTA after immersion in various soaking solutions such as phosphate-buffered saline (PBS), fetal bovine serum (FBS), hexadecane oil, and deionized water. The initial and final setting times were determined by testing with Gilmore needles of two different weights. Expansion was measured with a linear variable differential transformer device over 180 minutes, starting 30 minutes after the materials were mixed. For this initial 30 minutes prior to immersion, the samples were stored at 37° and 50% relative humidity for the cement to set enough to resist breakdown of the cement surface by the probe. The initial 30 minutes set time was determined in pilot studies. Gray MTA was measured to have an initial setting time of 41 minutes and a final setting time of 170 minutes.

The expansion of gray MTA was 0.77% in water, 1.04% in PBS, 0.07% in 80% PBS/20% FBS. Gray MTA immersed in hexadecane shrank 0.15%. The 80% PBS/20% FBS solution was used to mimic body fluids. Samples in this fluid demonstrated a greater effect than would be expect: 93% reduction in expansion versus the expected 20% consistent with the percentage of reduced water available. The authors propose that the serum proteins adsorbed to the gray MTA and reduced the dimensions of the surface porosites. In the absence of water, the hexadecane oil group, the material demonstrated

shrinkage which may have been a result of dehydration from the oil (Gandolfi et al., 2009). The mean shrinkage of white MTA of 1.84% measured in the current study may be an indication of inadequate humidity in the setting environment, when compared to other studies that demonstrated expansion. The shrinkage of white MTA in the current study was greater than the shrinkage of the gray MTA immersed in hexadecane oil in the study by Gandolfi et al. (2009). This may be due to the 30-minute delay for initial setting of the materials prior to starting the measurements in the previous study. There may have been dimensional changes prior to the measurement beginning, leading to an underestimation of the shrinkage in an environment with inadequate water available to the material. An advantage to Digital Image Correlation is not needing to contact the surface which is being measured, where the previous study needed an initial set in order for the material surface to resist breakdown by the probe that was being used to measure the expansion.

In the current study, Biodentine had a mean shrinkage of 1.3% at the 60-minute time point. Camilleri (2014) reported shrinkage of Biodentine when setting in a dry environment and also when stored in Hank's Balanced Salt Solution. Root dentin to material interface assessment in a dry environment showed a marginal gap of 1-2 μm formed between the dentine and Biodentine, as a result of the Biodentine drying out. This resulted in shrinkage and also crack formation parallel to the dentinal walls. Biodentine stored in Hank's Balanced Salt Solution resulted in a gap of 2 μm at the dentine-material interface. The authors recommended that the tricalcium silicate materials be kept moist when used clinically, as drying out of the material leads to

shrinkage and cracking of the material (Camilleri et al., 2014). At the final Biodentine measurement, at 60 minutes, the material appears to still be undergoing dimensional changes; however, the material was hard enough set that it had to be removed from the mold using a high speed handpiece.

EndoSequence Root Repair Material expanded a mean of 1.23% at the 4-hour measurement, the completion of the experiment, within the confines of this experimental model. At this time point, the material appears to still be undergoing dimensional changes. The measurements were ended at four hours due to the previously described surface sheen which at longer time points created too much artifact to be able to measure the dimensional changes accurately. In a cytotoxicity study, it was noted that neither the ERRM putty nor paste set in a 100% humidity and 37°C environment until 168 hours, which was assessed by the material being able to withstand a 500-g load (Damas et al., 2011). Another study looked at the setting time of gray MTA and ERRM in the presence of blood or Minimum Essential Media (MEM; Sigma-Aldrich, St. Louis, MO). There was a dry control of each material, a wet control submerged in sterile saline and experimental groups submerged in blood, MEM, or a combination of the two fluids. There was not a difference in setting between the different media; however, at the 48-hour time point, none of the ERRM samples were set (Charland et al., 2013). Lovato et al. (2011) noted difficulty in getting a complete set of the EndoSequence materials, and that the set began only when the materials were completely covered by water.

The bioceramic materials set via a hydration reaction; thus, the water available during the setting time is a critical part of the final properties of the material. With

adequate water present, the bioceramic materials will expand; however, shrinkage has been observed in this study and previous studies in a drier environment. In the surgical setting, the root-end filling is not submerged in saline or water, but in body fluids. It is possible that our root-end restorations could shrink upon setting in clinical use. This is especially something to consider if biocermic materials are used to obturate the full length of a canal, where the fluid available would be limited to the dentinal tubules along the length.

The current methodology resulted in an inadequate amount of water available for the complete hydration of the bioceramic cements. In this study, water might only contact one surface of the cement as the other surfaces where covered by the mold, and the humidity was likely not maintained adequately elevated as images were taken. The constraints of the mold were also likely to have led to underestimates of the dimensional changes of materials that expand. A follow-up study could be done using dentin disks from extracted human or bovine teeth. The dentinal tubules would allow greater hydration to reach the cement. The concern with expansion of the root end filling material is risk of fracture of the root secondary to the expansion. Measurement of the expansion of a dentin disk, or root fragment, could be done by placing a strain gauge on the surface of the dentin. This would be a more direct method of evaluating the strain in the dentin due to the expanding bioceramic material, and it would allow immersion of the samples in different media, ensuring adequate hydration and allowing comparison of environments.

Conclusions

The water available during the setting of Mineral Trioxide Aggregate, EndoSequence Root Repair Material, and Biodentine has an effect on the dimensional changes of the material. White MTA and Biodentine have previously been shown to expand with adequate hydration, but may shrink in an environment that is drier. Bioceramic materials should be mixed according to the manufacturer's directions, and should be kept moist while setting to ensure complete hydration of the cements and prevention of shrinkage. Further research is needed to determine if the dimensional changes during setting of bioceramic materials increases the risk of root fracture.

References

AAE Endodontics: Colleagues for Excellence Fall 2010.

Abou-Rass M, Frank AL, Glick DH. The anticurvature filing method to prepare the curved root canal. J Am Dent Assoc 1980;101:792-794.

Active Biosilicate Technology ™, Septodont: Biodentine ™ scientific file. Saint-Maur-des-Fossés Cedex, France: R&D Department, 2010.

AlAnezi AZ, Jiang J, Safavi KE, Spangberg LSW, Zhu Q. Cytotoxicity evaluation of endosequence root repair material. Oral Surg Oral Med Oral Pathol Oral Radiol Endod 2010;109:e122-e125.

Alhadainy HA. Root perforations: a review of the literature. Oral Surg Oral Med Oral Pathol 1994;78:368-374.

Bargholz C. Perforation repair with mineral trioxide aggregate: a modified matrix concept. Int Endod J 2005;38:59-69.

Benenati FW, Roane JB, Biggs JT, Simon JH. Recall evaluation of iatrogenic root perforations repaired with amalgam and gutta-percha. J Endod 1986;12:161-166.

Bozeman BT, Lemon RR, Eleazer P. Elemental analysis of crystal precipitate from Gray and White MTA. J Endod 2006;32:425-428.

Camilleri J. Characterization of hydration products of mineral trioxide aggregate. Int J Endod 2008;41:408-417.

Camilleri J. Hydration mechanisms of mineral trioxide aggregate. Int J Endod 2007;40:462-470.

Camilleri J, Grech L, Galea K, Keir D, Fenech M, Formosa L, Damidot D, Mallia B. Porosity and root dentine to material interface assessment of calcium silicate-based root-end filling materials. Clin Oral Invest 2014;18:1437-1446.

Camilleri J, Montesin FE, Brady K, Sweeney R, Curtis RV, Pitt Ford TR. The constitution of mineral trioxide aggregate. Dent Mater 2005;21:297-303.

Camilleri J, Montesin FE, Papaioannou S, McDonald F, Pitt Ford TR. Biocompatibility of two commercial forms of mineral trioxide aggregate. Int J Endod 2004;37:699-704.

Camilleri J, Pitt Ford TR. Mineral trioxide aggregate: a review of the constituents and biological properties of the material. Int J Endod 2006;39:747-754.

Camilleri J, Sorrentine F, Damidot D. Investigation of the hydration and bioactivity of radiopacified tricalcium silicate cement, Biodentine and MTA Angelus. Dent Mater 2013;29:580-593.

Charland T, Hartwell GR, Hirschberg C, Patel R. An evaluation of setting time of Mineral Trioxide Aggregate and EndoSequence Root Repair Material in the presence of human blood and essential media. J Endod 2013;39:1071-1071.

Chen I, Karabucak B, Wang C, Wang HG, Koyama E, Kohli MR, Nah HD, Kim S. Healing after root-end microsurgery by using mineral trioxide aggregate and a new calcium silicate-based bioceramic material as root-end filling materials in dogs. J Endod 2015;41:389-399.

Chng HK, Islam I, Yap AU, Tong YW, Koh ET. Properties of a new root-end filling material. J Endod 2005;31:665-668.

Chuang SF, Chang CH, Chen TY. Spatially resolved assessments of composite shrinkage in MOD restorations using a digital-image-correlation technique. Dent Mater 2011;27:134–143.

Chuang S, Chen T, and Chang C. Application of digital image correlation method to study dental composite shrinkage. Strain 2008;44:231-238.

Damas B.A., Wheater M.A., Bringas J.S. Cytotoxicity comparison of Mineral Trioxide Aggregates and EndoSequence Bioceramic Root Repair Materials. J Endod 2011;37:372-375.

Frank AL. Resorption, perforations, and fractures. Dent Clin North Am 1974;18:465-488.

Gandolfi MG, Iacono F, Agee K, Siboni F, Tay F, Pashley DH, Prati C. Setting time and expansion in different soaking media of experimental accelerated calcium-silicate cements and ProRoot MTA. Oral Surg Oral Med Oral Pathol Oral Radiol Endod 2009;108:e39-e45.

Grech L, Mallia B, Camilleri J. Characterization of set Intermediate Restorative Material, Biodentine, Bioaggragate and a prototype cacium silicate cement for use as root-end filling materials. Int J Endod 2013;46:632-641.

Grech L, Mallia B, Camilleri J. Investigation of the physical properties of tricalcium silicate cement-based root-end filling materials. Dent Mater 2013;29:e20-e28.

Hansen SW, Marshall JG, Sedgley CM. Comparison of intracanal EndoSequence Root Repair Material and ProRoot MTA to induce pH changes in simulated root resorption defects over 4 weeks in matched pairs of human teeth. J Endod 2011;37:502-506.

Harris SP, Bowles WR, Fok A, McClanahan SB. An anatomic investigation of the mandibular first molar using micro-computed tomography. J Endod 2013;39:1374-1378.

Hirschman, W.R., Wheater, M., Bringas, J. et al. Pulp-capping agents with a new bioceramic root repair putty. J Endod 2012;38:385–388.

Jafarzadeh H, Abbott PV. Ledge formation: Review of a great challenge in endodontics. J Endod 2007;33:1155-1162.

Johnson BR. Considerations in the selection of a root-end filling material. Oral Surg Oral Med Oral Pathol Oral Radiol Endod 1999;87:398-404.

Kakehashi S, Stanley HR, Fitzgerald RJ. The effects of surgical exposures of dental pulps in germ-free and conventional laboratory rats. Oral Surg Oral Med Oral Pathol 1965;20:340-348.

Kang JD, Ososkov Y, Embury JD, Wilkinson DS. Digital image correlation studies for microscopic strain distribution and damage in dual phase steels. Scripta Materialia 2007;56:999–1002.

Kim S. Color atlas of microsurgery in endodontics. W.B. Saunders Company. Harcourt Health Sciences Company, 2001.

Kim S, Kratchman S. Modern endodontic surgery concepts and practice: a review. J Endod 2006;32:601-623.

Kim, Y., Kim, S., Shin, Y. et al. Failure of setting of mineral trioxide aggregate in the presence of fetal bovine serum and its prevention. J Endod 2012;34:536–540.

Lau A, Li J, Heo YC, Fok A. A study of polymerization shrinkage kinetics using digital image correlation. Dent Mater 2015;31;391-398.

Lemon RR. Nonsurgical repair of perforation defects: internal matrix concept. Dent Clin North Am 1992;36:439-458.

Li J, Fok ASL, Satterthwaite J, Watts DC. Measurement of the full-field polymerization shrinkage and depth of cure of dental composites using digital image correlation. Dent Mater 2009(a);25:582-588.

Li J, Li H, Fok AS, Watts DC. Multiple correlations of material parameters of light-cured dental composites. Dent Mater 2009(b);25:829–836.

Li J, Thakur P, Fok ASL. Shrinkage of Dental Composite in Simulated Cavity Measured with Digital Image Correlation. J Vis Exp 2014;(89), e51191, doi:10.3791/51191.

Lovato KF, Sedgley CM. Antibacterial activity of EndoSequence Root Repair Material and ProRoot MTA against clinical isolates of *Enterococcus faecalis.* J Endod 2011;37:1542-1546.

Ma J, Shen Y, Stojicic S, Haapasalo M. Biocompatibility of two novel root repair materials. J Endod 2011;37:793-798.

McCormick N, Lord J. Digital Image Correlation. Mater Today 2010;13:52-54.

Miletic V, Manoilovic D, Milosevic M, Mitrovic N, Stankovic TS, Maneski T. Analysis of local shrinkage patterns of self-adhering and flowable composites using 3D digital image correlation. Quintessence Int 2011;42(9):797-804.

Parirokh M, Torabinejad M. Mineral trioxide aggregate: a comprehensive literature review—part I: chemical, physical and antibacterial properties. J Endod 2010;36:16-27.

Parirokh M, Torabinejad M. Mineral trioxide aggregate: a comprehensive literature review—part III: clinical applications, drawbacks, and mechanism of action. J Endod 2010;36:400-13.

Pitt Ford TR, Torabinejad M, McKendry DJ, Hong C, Kariyawasam SP. Use of mineral trioxide aggregate for repair of furcal perforation. Oral Surg Oral Med Oral Pathol Oral Radiol Endod 1995;79:756-763.

Rifaey HS, Villa M, Zhu Q, Wang YH, Safavi K, Chen IP. Comparison of the osteogenic potential of Mineral Trioxide Aggregate and EndoSequence Root Repair Material in a 3-dimensional culture system. J Endod 2016;42:760-765.

Schilder H. Cleaning and shaping the root canal. Dent Clin North Am. 1974;18:269-96.

Shokouhinejad, N., Nekoofar, M.H., Razmi, H. et al. Bioactivity of EndoSequence root repair material and bioaggregate. Int Endod J 2012;45 1127–1134.

Simon JHS. The apex: how critical is it? Gen Dent 1994;42:330-334.

Song JS, Mante FK, Romanow WJ, Kim S. Chemical analysis of powder and set forms of Portland cement, gray ProRoot MTA, white ProRoot MTA, and gray MTA-Angelus. Oral Surg Oral Med Oral Pathol Oral Radiol Endod 2006;102:809-815.

Storm B, Eichmiller FC, Tordik PA, Goodell GG. Setting expansion of gray and white mineral trioxide aggragate and Portland cement. J Endod 2008;34:80-82.

Torabinejad M, Hong CU, Lee SJ, Monsef M, Pitt Ford TR. Investigation of mineral triaggregate for root-end filling in dogs. J Endod 1995;21:603-608.

Torabinejad M, Parirokh M. Mineral trioxide aggregate: a comprehensive literature review—part II: leakage and biocompatibility. J Endod 2010;36:190–202.

Tsesis I, Fuss Z. Diagnosis and treatment of accidental root perforations. Endod Topics 2006;13:95-107.

Walsh R.M., Woodmansy K.F., Glickman G.N. Evaluation of compressive strength of hydraulic silicate-based root-end filling materials. J Endod 2014;40:969-972.

Weine FS, Kelly RF, Lio PJ. The effect of preparation procedures on original canal shape and on apical foramen shape. J Endod 1975;1:255-262.

Zanini M.,Sautier J.M., Berdal A. et al. Biodentine Induces Immortalized Murine Pulp Cell Differentiation into Odontoblast-like Cells and Stimulates Biomineralization. J Endod 2012;38:1220-1226.

Zhou H., Shen Y., Wang Z. et al. In Vitro Cytotoxicity Evaluation of a Novel Root Repair Material. J Endod 2013;39:478-483.

Zhu Q, Safavi KE, Spangberg LSW. Cytotoxic evaluation of root-end filling materials in cultures of human osteoblast-like cells and periodontal ligament cells. J Endod 1999;25:410-412.

Appendix

MTA

Time (min)	1		2		3		4		5	
	Exx	Eyy	Exx	Eyy	Exx	Eyy	Exx	Eyy	Exx	Eyy
15	-0.28912	-0.34248			-1.62673	-1.16599	-0.92227	-1.09836	-1.06007	-1.09381
30	-0.32257	-0.40828	-0.84500	-0.66173	-1.68243	-1.21335	-1.01425	-1.16359	-1.12519	-1.17173
45	-0.35901	-0.41834	-0.90762	-0.73203	-1.69270	-1.20624	-1.00242	-1.21141	-1.15196	-1.16537
60	-0.36712	-0.43689	-0.92982	-0.73485	-1.69934	-1.22816	-1.08934	-1.22424	-1.15008	-1.18552
120	-0.38164	-0.45789	-0.94426	-0.73630	-1.71703	-1.24915	-1.04371	-1.20939	-1.18139	-1.22012
180	-0.39832	-0.45573	-0.96003	-0.76601	-1.72086	-1.24407	-1.05355	-1.23104	-1.18380	-1.21831
240	-0.39124	-0.46669	-0.97036	-0.77683	-1.72721	-1.25230	-1.07043	-1.23813	-1.19352	-1.22785

Time (min)	6		7		8		9		10	
	Exx	Eyy	Exx	Eyy	Exx	Eyy	Exx	Eyy	Exx	Eyy
15	-0.56421	-0.575776	-0.777319	-0.859111	-0.652487	-0.81592	-0.652487	-0.815923	-0.608202	-0.445924
30	-0.61423	-0.610582	-0.875946	-0.937726	-0.709184	-0.86169	-0.709184	-0.861690	-0.692404	-0.52579
45	-0.61027	-0.619384	-0.895214	-0.931624	-0.762761	-0.91331	-0.762761	-0.913306	-0.70686	-0.52155
60	-0.62821	-0.645468	-0.859848	-0.875331	-0.732968	-0.88329	-0.732968	-0.88329	-0.68989	-0.50063
120	-0.64109	-0.645667	-0.926680	-0.938939	-0.492700	-0.90671	-0.749270	-0.90671	-0.75464	-0.57818
180	-0.65227	-0.672823	-0.974850	-0.976436	-0.721610	-0.93238	-0.77216	-0.93238	-0.75834	-0.60526
240	-0.65563	-0.657306	-0.994674	-1.024690	-0.77561	-0.932	-0.77561	-0.93200	-0.75243	-0.61942

Table 8: Strain in x and y planes, Exx and Eyy, analyzed at each time point for each white MTA sample. *Note: in sample 2 at 15 min the computer froze and the image was not recorded.

ERRM

Time (min)	1		2		3		4		5	
	Exx	Eyy	Exx	Eyy	Exx	Eyy	Exx	Eyy	Exx	Eyy
15	0.040786	0.045224	0.065305	0.076252	-0.001616	0.088126	-0.003564	-0.003810	0.080153	0.069284
30	0.053611	0.061951	0.081277	0.118033	0.038704	0.126969	0.009241	-0.046251	0.072468	0.042478
45	0.052978	0.061740	0.088124	0.134096	0.047997	0.166692	0.054001	0.061205	0.083378	0.053514
60	0.045657	0.056321	0.119124	0.176272	0.088981	0.198167	0.041475	0.043388	0.066081	0.050511
120	0.041723	0.072178	0.154127	0.213312	0.215845	0.405006	0.086569	0.086183	0.128683	0.075630
180	0.048427	0.090193	0.211865	0.281795	0.434350	0.688952	0.110668	0.182186	0.185067	0.115076
240	0.063697	0.109484	0.390476	0.493309	0.662886	0.870628	0.205096	0.259299	0.249229	0.163236

Time (min)	6		7		8		9		10	
	Exx	Eyy	Exx	Eyy	Exx	Eyy	Exx	Eyy	Exx	Eyy
15	0.015283	0.049473	0.101079	0.122500	0.011002	0.090022	0.188937	0.167327	0.085377	0.085032
30	0.031831	0.076664	0.204462	0.252222	-0.010531	0.171082	0.282593	0.245481	0.227983	0.225436
45	0.058909	0.112870	0.282676	0.333460	0.041866	0.173567	0.330201	0.259194	0.244596	0.236360
60	0.019644	0.073612	0.350567	0.417245	0.172555	0.239535	0.381040	0.276895	0.257662	0.232058
120	0.108379	0.102280	0.578628	0.671330	0.508068	0.525773	0.731470	0.561846	0.420573	0.385374
180	0.154075	0.123440	0.952815	1.112350	0.870885	0.996013	0.959914	0.704649	0.664218	0.645561
240	0.209998	0.271816	1.173350	1.381740	1.151770	1.329030	1.071980	0.831105	0.698189	0.675159

Table 9: Strain in x and y planes, Exx and Eyy, analyzed at each time point for each ERRM sample.

		Biodentine									
		1		2		3		4		5	
		Exx	Eyy	Exx	Eyy	Exx	Eyy	Exx	Eyy	Exx	Eyy
Time (min)	15	-0.22636	-0.22298	-0.38593	-0.14585	-0.2838	-0.26376	-0.19611	-0.24784	-0.44925	-0.32705
	30	-0.24028	-0.29449	-0.60453	-0.52813	-0.51641	-0.49569	-0.32314	-0.3737	-0.63451	-0.61645
	45	-0.46783	-0.46846	-0.65395	-0.59454	-0.73636	-0.70794	-0.46348	-0.50732	-0.78329	-0.74993
	60	-0.58159	-0.62702	-0.76909	-0.51138	-0.88641	-0.84676	-0.56118	-0.59871	-0.9173	-0.96092
		6		7		8		9		10	
		Exx	Eyy	Exx	Eyy	Exx	Eyy	Exx	Eyy	Exx	Eyy
Time (min)	15	-0.09971	-0.19827	-0.17184	-0.1749	-0.2212	-0.29482	-0.1284	-0.09001	-0.03318	-0.0298
	30	-0.22751	-0.33324	-0.27389	-0.27663	-0.24044	-0.26095	-0.32705	-0.34733	-0.05142	-0.07547
	45	-0.36021	-0.46115	-0.53305	-0.40878	-0.5932	-0.35704	-0.57243	-0.66539	-0.08574	-0.13897
	60	-0.43656	-0.5312	-0.69136	-0.61449	-0.65859	-0.75351	-0.80557	-0.84033	-0.16097	-0.26551

Table 10: Strain in x and y planes, Exx and Eyy, analyzed at each time point for each Biodentine sample.